35th EPS Conference on Plasma Phys. Hersonissos, 9 - 13 June 2008 ECA Vol.**32D**, P-2.060 (2008)

KINETIC EFFECTS OF ENERGETIC PARTICLES ON RESISTIVE MHD STABILITY

Ryoji Takahashi[1], Dylan P. Brennan[1], Charlson C. Kim[2]

[1]*Department of Physics and Engineering Physics, The University of Tulsa, 800 South Tucker Drive, Tulsa, OK 74104*

[2]*Plasma Science and Innovation Center, The University of Washington, Seattle, WA 98195*

Introduction

It is conjectured that kinetic effects of energetic particles can play a crucial role in the stability of the 2/1 tearing mode in tokamaks such as JET, JT-60U, and DIII-D, where the fraction of energetic particles β is high (where $\beta = 2\mu_0 P/B^2$, P is pressure, B is magnetic field). The energetic particle stabilization of the internal kink mode has been studied extensively, and the stabilization comes from conservation of an effective total perturbed potential energy when the energetic particles precession frequency is much larger than the MHD growth rate [2]. In this work, we examine energetic particle effects on the non-ideal MHD linear stability and nonlinear evolution of cases unstable to the 2/1 mode. Using model equilibria based on DIII-D experimental reconstructions, the non-ideal MHD linear stability and nonlinear evolution of these cases are investigated by using the nonlinear 3-D resistive MHD code NIMROD [1]. Energetic particle effects are investigated by a δf PIC model coupled to the MHD solution in the NIMROD code. This hybrid kinetic-MHD model was used to study kinetic effects on the 1/1 internal kink mode [3]. Here, this model is applied to the linear stability and nonlinear evolution of these cases, and it has been observed that the energetic particles have a significant effect on the stability of the 2/1 mode. The growth rates of the 2/1 mode are calculated as a function of Lundquist number S = $\tau_R/\tau_A > 10^5$ (the ratio of the resistive time to Alfvén time), in the asymptotic regime. The growth rates reduce with energetic particle β fraction due to flattening of the particle distribution function in the resonance region. Furthermore, the study of energetic particle effects on MHD modes is important for ITER operation, where S and energetic β fraction will exceed current experiments.

Our methods

NIMROD solves the linear and nonlinear MHD equations by initial value computations with a mesh of finite elements for the poloidal ($R-Z$) plane and finite Fourier series for the toroidal

direction. The time advance is described by [1]. The single fluid form of the equations is

$$\begin{aligned} \rho(\frac{\partial V}{\partial t}+V\cdot\nabla V) &= J\times B-\nabla-p\nabla\cdot\Pi, \\ E &= -V\times B+\eta J, \\ n\frac{\partial T}{\partial t}+V\cdot\nabla T+(\Gamma-1)nT\nabla\cdot V &= -(\Gamma-1)\nabla\cdot q+(\Gamma-1)Q, \\ q &= -(\kappa_{\|}-\kappa_{\perp})\nabla_{\|}T-\kappa_{\perp}\nabla T, \end{aligned} \tag{1}$$

along with Maxwell's and continuity equations, where ρ is the mass density, J is the current density, B is the magnetic field p is the pressure, Π is the stress tensor (including a numerical $-\rho\nu\nabla^2 V$). E is the electric field, η is the electric resistivity, T is the temperature, Γ is the ratio of specific heats, q is the heat flux, and κ is the thermal diffusivity.

The Hyper Kinetic Model is assumed where the density of energetic particles (n_h) is negligible compared to the bulk MHD density (n_0): ($n_h \ll n_0$) but energetic particle β_h is on the order of the bulk plasma β_0: ($\beta_h \sim \beta_0$). In this approximation, any energetic particle species contribution to the center of mass velocity is neglected. However, the energetic species modifies the momentum equation (1) with an additional energetic ion pressure tensor p_h as

$$\rho(\frac{\partial V}{\partial t}+V\cdot\nabla V)=J\times B+\nabla\cdot\rho\nu\nabla V-\nabla p_b-\nabla\cdot p_h, \tag{2}$$

where p_h is the background pressure tensor. p_h is assembled from a PIC δf method (where f is the velocity distribution function over the computational grid and $f = f_{eq}+\delta f$, where f_{eq} is the equilibrium or steady state distribution) and at each timestep $p_h = p_{h0}+\delta p$. Notice that the steady state fields satisfy a scalar pressure force balance which limits the form of the equilibrium energetic particle distribution to isotropic distributions in velocity. This implies

$$\delta p=\int m(v-v_h)^2\delta f(r,v)d^3v \tag{3}$$

is integrated over the volume.

δf PIC evolves along the phase space characteristics (or trajectories) using the Vlasov equation

$$\frac{\partial f}{\partial t}+\dot{z}\frac{\partial f}{\partial z}=0, \tag{4}$$

where z as the generic (6D) phase space coordinate. Then the drift kinetic equations can be described by

$$\frac{\partial x}{\partial t}=v_{\|}\hat{b}+\frac{m}{eB^4}(v_{\|}^2+\frac{v_{\perp}^2}{2})(B_0\times\nabla\frac{B_0^2}{2})+\frac{\mu_0 m v_{\|}^2}{eB_0^2}J_{\perp 0},$$

where $m\dot{v}_{\|}=-\hat{b}_0\cdot(\mu\nabla B-eE)$ and $z=(x_{gc},\mu,v_{\|})$ where x_{gc} is the guiding center coordinate. All detailed descriptions and implementations of the code can be found in Ref. [3].

Equilibria are constructed as described by Ref. [4]: The profiles are the gradient in P approaching zero near the edge, while the q profile and zero-dimensional parameters approach those of the experiment with β_N near the $(m/n = 2/1)$ ideal kink limit. This allows for lower local gradients in the pedestal region, while still reaching large values of β.

Results and Discussions

First, the linear instability of a sequence of equilibria is investigated with and without the energetic particles.

Fig. 1 shows the growth rates of linear calculations versus $\beta_N/4l_i$ with different energetic particle fractions β_{frac}, and shows contours of a fixed linear growth rate $\gamma = 1.0 \times 10^4$ with different β_{frac}. All calculations are performed at the Prandtl number, $Pr =$ (kinetic viscosity, ν /electric diffusivity , η), is 100 and different Ss. The x axis is S, the y axis is $\beta_N/4l_i$, and the z axis is the growth rates. The red, the blue, the light blue, and the black planes show the linear growth rate as a function of S and a function of $\beta_N/4l_i$ with $\beta_{frac} = 0.0$, 0.25, 0.5, and 0.75 respectively. The growth rates are damped for higher energetic particle fractions. The green, pink, yellow, and red contour lines are a fixed growth rate $\gamma = 1.0 \times 10^4$ with $\beta_{frac} = 0.0$, 0.25, 0.5, and 0.75 respectively. At lower $\beta_N/4l_i$, i.e. pressure, are found stable cases. However, the energetic particles are clearly damping as the contour of fixed $\gamma = 1.0 \times 10^4$ moves to high S and $\beta_N/4l_i$. Stability boundaries are found at low $\beta_N/4l_i$ and at low and high S, however these are computationally expensive to calculate in detail. The effect on the stability boundary is being investigated.

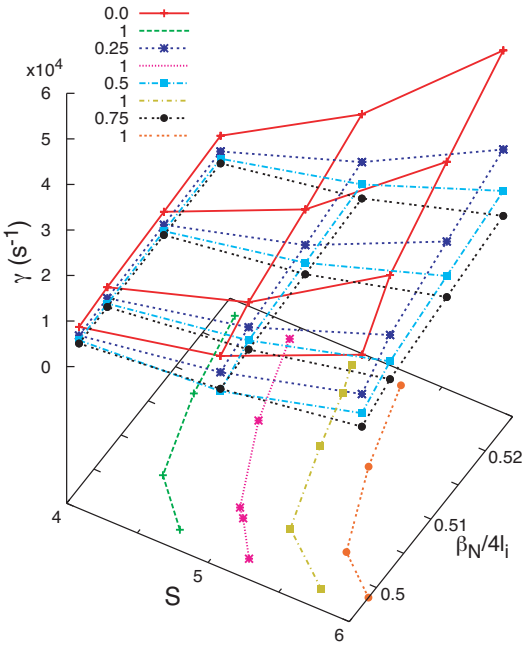

Figure 1: The growth rate of linear calculations and fixed growth rate $\gamma = 1.0 \times 10^4$ contours with different energetic particle fractions as a function of S and $\beta_N/4l_i$.

With 11 modes, nonlinear calculations are performed with $S = 10^6$ and $\beta_N/4l_i = 0.4973$. In order to study the energetic particle effects, one is performed with MHD only, and the other with $\beta_{frac} = 0.5$. Except for the energetic particle fraction, both calculations are identical. In the nonlinear calculation, at the beginning of the linear phase, the growth rates are damped by the trapped energetic particle fraction. However, the energetic particle fraction

interaction at the later stage of the nonlinear phase is not trivial. Further studies of nonlinear calculations with the energetic particles will be reported in future publications. Here, we would like to show the highlights of how nonlinear calculations with energetic particle fractions have different features compared with linear cases.

FIg. 2 shows the phase space δf of energetic particles in the nonlinear driven phase (a) and mode saturation phase (b). During the linear growth of evolution, it has a full trapped cone structure, then at saturation in the nonlinear regime (a), the phase space is similar to the linear calculation (not shown).

Notice that at the later stage of saturation $Re(\delta f)$ has a double trapped cone's structure. Compared with the nonlinear pure MHD results, it is not trivial to see the detailed mechanism of the effect of energetic particle fractions in the nonlinear stages. Consideration of the island structure is important in understanding the energetic particle effects.

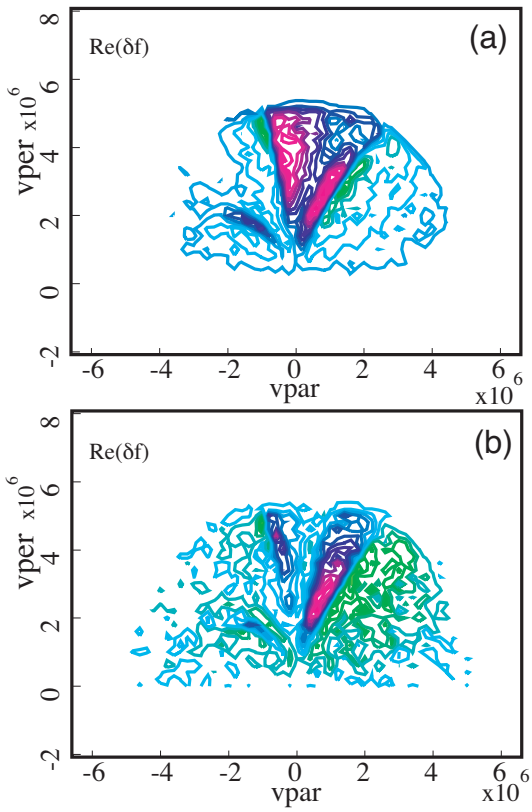

Figure 2: The phase space δf of energetic particles in the nonlinear driven phase (a) and mode saturation phase (b) in the nonlinear calculations

Acknowledgments: R. Takahashi is supported by US DOE Grant DE-FG02-07ER54931.

References

[1] C. Sovinec *et al.*, J. Comp. Phys. **195**, 355 (2004).

[2] F. Porcelli, Plasma Phys. Controlled Fusion **1601**, 1601 (1991).

[3] C. Kim, C. Sovinec, and S. Paker, Comput. Phys. Comm **164**, 448 (2004).

[4] D. P. Brennan, S. E. Kruger, T. A. Gianakon, and D. D. Schnack, Nucl. Fusion **45**, 1178 (2005).